Physics Letters B 687 (2010) 305–309

Contents lists available at ScienceDirect

Physics Letters B

www.elsevier.com/locate/physletb

g Factor of the 7^- isomer in ^{126}Sn and first observation of spin-alignment in relativistic fission

G. Ilie [a,b,*,1], G. Neyens [c], G.S. Simpson [d,e], J. Jolie [a], A. Blazhev [a], H. Grawe [f], R.L. Lozeva [c,g], N. Vermeulen [c], L. Atanasova [g], D.L. Balabanski [h,i], F. Becker [f], P. Bednarczyk [f,j], C. Brandau [f,k], L. Caceres [f,l], S.K. Chamoli [m], J.M. Daugas [n], P. Doornenbal [f], J. Gerl [f], M. Górska [f], J. Grębosz [f,j], M. Hass [m], M. Ionescu-Bujor [b], A. Jungclaus [l], M. Kmiecik [j], I. Kojouharov [f], N. Kurz [f], A. Maj [j], S. Mallion [c], O. Perru [n], M. Pfützner [o], Zs. Podolyák [k], W. Prokopowicz [f], M. De Rydt [c], T.R. Saito [f], H. Schaffner [f], K. Turzó [c], J. Walker [k], E. Werner-Malento [f], H.J. Wollersheim [f]

[a] IKP, Universität zu Köln, 50937 Köln, Germany
[b] National Institute for Physics and Nuclear Engineering, 76900 Bucharest, Romania
[c] Instituut voor Kern- en Stralingsfysica, K.U. Leuven, 3001 Leuven, Belgium
[d] ILL, 38042 Grenoble Cedex, France
[e] LPSC, Université Joseph Fourier Grenoble 1, CNRS/IN2P3, INPG, 38026 Grenoble Cedex, France
[f] GSI, 64291 Darmstadt, Germany
[g] Faculty of Physics, University of Sofia "St. Kl. Ohridski", 1164 Sofia, Bulgaria
[h] Dipartimento di Fisica, Universitá di Camerino, 62032 Camerino, Italy
[i] INRNE, Bulgarian Academy of Sciences, 1784 Sofia, Bulgaria
[j] The Henryk Niewodniczański Institute of Nuclear Physics, PAN, 31342 Kraków, Poland
[k] Department of Physics, University of Surrey, Guildford, GU2 7XH, UK
[l] Departamento de Fisica Teórica, Universidad Autonoma de Madrid, 28049 Madrid, Spain
[m] Department of Particle Physics, Weizmann Institute of Science, 76
[n] CEA, DAM, DIF, 91297 Arpajon Cedex, France
[o] IEP, Warsaw University, 00681 Warsaw, Poland

ARTICLE INFO

Article history:
Received 6 October 2009
Received in revised form 17 February 2010
Accepted 9 March 2010
Available online 16 March 2010
Editor: V. Metag

Keywords:
Nuclear moments
Lifetimes
Shell model calculations
Projectile fission reactions

ABSTRACT

We report on the g factor measurement of the isomeric 7^- state ($E^* = 2219$ keV, $T_{1/2} = 5.9(8)$ µs) in the neutron-rich ^{126}Sn nucleus. The nucleus was produced by the fission of a relativistic ^{238}U beam and reaction products were selected by the FRS fragment separator at GSI. For the first time, spin-alignment was observed after relativistic fission. It was used to deduce the g factor of the 7^- isomeric state, $g(7^-) = -0.098(9)$, from the measured perturbed angular distribution of its γ decay using the RISING Cluster detectors. The observed value confirms the suggested $\nu(h_{11/2}^{-1}d_{3/2}^{-1})$ dominant configuration, which has been proposed for the 7^- isomers in neutron-rich Sn isotopes. The failure of the g factor additivity rule and the importance of core polarization evolution with increasing distance from the doubly-magic ^{132}Sn is discussed. The first observation of 18(8)% of spin-alignment produced by the relativistic fission of a ^{238}U beam paves the way to study moments of neutron-rich (sub-)microsecond isomers, which are difficult to align by other means.

The availability of beams of exotic radioactive nuclei for detailed spectroscopic studies, has allowed the observation of changes in the structure of atomic nuclei when going from stability, both to proton- and neutron-rich regions. Near the $Z = 50$ shell closure for example, the persistence of the $N = 82$ shell gap is being debated for neutron-rich isotopes below the doubly-magic ^{132}Sn [1–4]. Magnetic moments of isomeric states may serve as ideal probes to test nuclear models and effective shell-model interactions in this neutron-rich region near the r-process path. Many microsecond isomers have been observed in this region, mainly using neutron-induced fission reactions [5], β-decay [6] and more recently also using relativistic fission [4,7] and fragmentation [8]. Magnetic moments of high-spin isomeric states provide key information on the nature of their single-particle configuration, and can be directly compared to predictions with different models.

* Corresponding author.
E-mail address: gabriela.ilie@yale.edu (G. Ilie).
[1] Present address: WNSL, Yale University, New Haven, CT 06520, USA.

0370-2693
doi:10.1016/j.physletb.2010.03.033

In order to study electromagnetic moments of isomeric states, one needs spin-aligned nuclear ensembles. Through the observation of the rotation of the nuclear spin-aligned ensemble, as a time-dependent change of the γ-ray angular distribution (TDPAD) in a magnetic field, the nuclear g factor can be measured [9]. Spin-aligned isomeric nuclear states are produced in several types of nuclear reactions [10]. The difficulty is to maintain the alignment up to the implantation point in cases where in-flight selection is performed. At relativistic beam energies, the first observation of spin-alignment in isomeric beams was reported by Schmidt-Ott [11] using the projectile fragmentation reaction. For neutron-induced fission and relativistic fission reactions, alignment has not been observed yet and the reaction mechanism to produce oriented states via relativistic fission is not completely understood. However, spin-alignment is known to exist in spontaneous fission [12] and has been used to study the g factor of the 6^+ isomer in ^{134}Te [13].

The aim of the experiment reported here is to prove, for the first time, the presence of spin-alignment in projectile fission at relativistic energies. At the same time, the g factor of the 7^- isomeric state at 2219 keV in the neutron-rich isotope ^{126}Sn [6] was investigated. It is expected to be small due to the opposite sign of contributions by $d_{3/2}$ and $h_{11/2}$ neutrons in the leading $(d_{3/2}h_{11/2})_{7-}$ configuration. Therefore it provides a crucial probe for small components in the wave function and for studying core polarization evolution away from ^{132}Sn. The experiment was performed at the GSI facility, where a ^{238}U beam was accelerated up to 750 MeV/u by the SIS-18 synchrotron, with a mean intensity of 10^8 pps. The beam impinged on a 1 g/cm^2 ^{9}Be target placed at the entrance of the FRS spectrometer [14] operated in achromatic mode, allowing the selection of one charge state per element. A 221 mg/cm^2 Nb stripper foil was mounted behind the Be target in order to produce more than 99% of fully stripped fragments (as calculated with the LISE++ simulation code [15]). Fully stripped fragments are required to maintain the eventual reaction-induced spin-alignment during transport through the FRS [16].

The nuclei of interest were selected and identified in two stages. In the first part of the FRS spectrometer, a selection in the longitudinal momentum distribution was carried out, in order to select a spin-aligned ensemble of isomers. As it has been shown already in fragmentation, that the spin alignment in the selected ensemble can be understood by simple kinematical arguments, and is related to its longitudinal momentum [11,17,16,18]. Similar arguments can be used to understand how spin-alignment can be produced in a relativistic-fission reaction, considering the spin-alignment process that is known to exist in spontaneous fission [12]. In such a fission process, two fragments are emitted back to back with equal momenta in the center-of-mass system and their spins are preferentially oriented in a plane perpendicular to their emission direction. Thus if a cone of the ensemble of fragments emitted into 4π is selected, an oblate-aligned ensemble is obtained with the alignment symmetry axis along the emission direction [13]. When the fissioning nuclei have a relativistic energy, the fission fragments are emitted in a forward focussed cone, with a velocity that is spread around the beam velocity. Fragments with a lower/higher velocity correspond to fission products that were emitted anti-parallel/parallel to the beam direction. Thus by selecting the higher or lower part of the longitudinal momentum distribution of the fission fragments, an oblate spin-aligned ensemble could be obtained whereby the spins are aligned perpendicular to the beam direction. The FRS was tuned to select the higher part of this distribution on the group of fission fragments with $Z = 50$. Using the Monte Carlo simulation code MOCADI [19] the calculated kinematic properties of ^{126}Sn ions produced in the reaction are presented in Fig. 1. The longitudinal momentum distribution

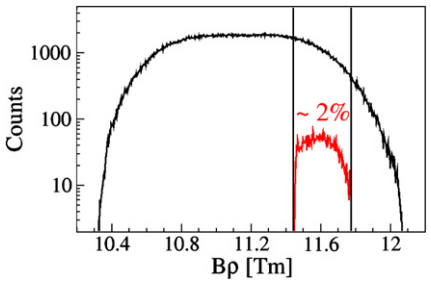

Fig. 1. MOCADI simulation of the distribution of the ^{126}Sn fragments after fission of ^{238}U at 750 MeV/nucleon. The acceptance of the FRS (red curve) is marked with a rectangular window. (For interpretation of the references to colour in this figure legend, the reader is referred to the web version of this Letter.)

of the fragments is proportional to the magnetic rigidity ($B\rho$) and was measured by a position-sensitive scintillator detector. In front of it, we keep the slits fully open. Fig. 1 simulates the total fission fragment longitudinal momentum distribution. The momentum acceptance of the FRS, which is only 2% of this total distribution, is indicated around the selected window. Fig. 1 illustrates the limitation of the spectrometer and the difficulty in selecting fission fragments. Based on previous studies a cut was made in the longitudinal momentum close to the maximum value of the magnetic rigidity ($B\rho$).

Once this momentum selection was performed, a further selection was accomplished using an achromatic Al wedge shaped degrader of 5 mg/cm^2 at the intermediate focal plane (more than 90% of the ions remained fully stripped after they passed this degrader). The identification of the reaction products in A/q and Z was performed in the second half of the FRS using the various detectors in the beam line, see [20] for details. The settings of the FRS allowed to select only fully stripped ions at the final focal point. The probability for electron pick-up in this final part of the beam line has been limited to less than 10% [21] by limiting the thickness of the final energy degrader just in front of the experimental set-up. After this degrader and before entering the set-up the beam intensity was 2.2×10^4 ions/s and the energy about 300 MeV/u. We expect a value for the isomeric ratio, around 10%, similar to the one obtained in [22]. In order to sufficiently reduce the beam energy prior to implantation in the Cu host, a 20 mm plexi-glass degrader has been fixed to the Cu stopper [16]. An air gap between the plexi-glass degrader and the stopper was avoided by putting a thin layer of grease between them. Thus the randomly oriented electron spins were decoupled from the nuclear spins as soon as the isomers reached the plexi-glass degrader and up to the implantation point in the Cu host, allowing to maintain the nuclear spin-alignment. Because the FRS is a zero-degree fragment separator, the spin-alignment symmetry axis is parallel to the beam axis at the implantation point [16]. The spin-aligned beam was implanted into an annealed high-purity 2 mm thick Cu foil (cubic lattice structure), placed between the poles of an electromagnet providing a vertical magnetic field of $B = 7000(10)G$, whose direction was periodically switched. A plastic scintillator at the focal plane of the FRS, placed upstream of the magnet, was used to provide the $t = 0$ signal for the γ-decay measurement, based on an event-by-event ion–gamma correlation [16]. The isomeric γ decays were measured during a 16 µs time window by the RISING array composed of eight former EUROBALL Cluster detectors [23], each containing seven encapsulated HPGe crystals. Each crystal had a relative efficiency of $\sim 60\%$ and an energy resolution of ~ 2 keV at 1332 keV. The detectors were placed in the horizontal plane at ± 45, ± 75, ± 105 and ± 135 degrees relative to the beam direction. The prompt atomic background radiation was eliminated from the γ-spectra by placing a hardware gate of 600 ns, thus making

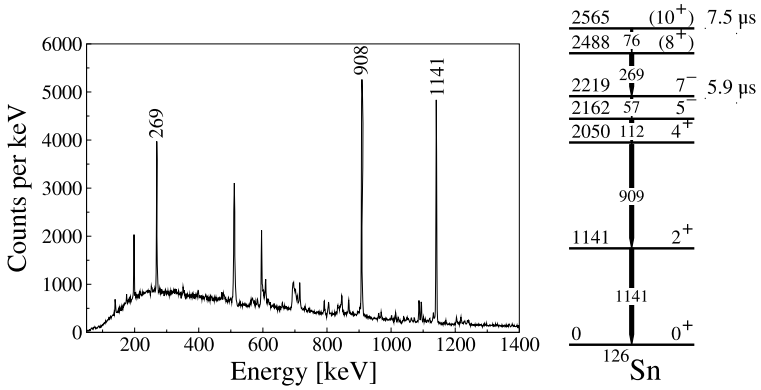

Fig. 2. The measured γ rays emitted after the decay of the isomeric states in ^{126}Sn (left) and the partial level scheme (right).

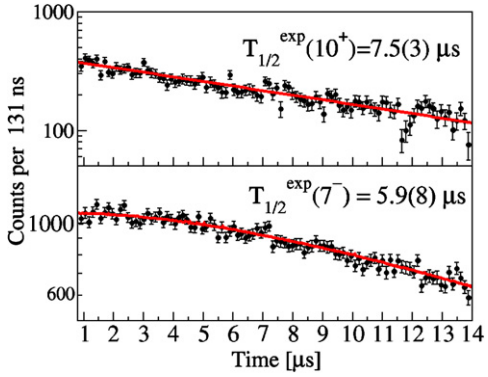

Fig. 3. (Color online.) Time distribution of the γ rays deexciting the isomeric levels in ^{126}Sn. Top: For the 269 keV line. Bottom: For the sum of γ rays with energies 909 keV and 1141 keV.

time analysis prior to this time impossible. More details on the experimental set-up and measuring procedure can be found in [21], while information of the data taking and analysis procedures are described in [20]. Data was analyzed using the Spy/Cracow software [24].

Two previously known microsecond isomeric states in ^{126}Sn have been populated (Fig. 2) [6,25]. Decay curves are obtained from the γ-time matrix by subtracting from each peak-decay curve a time spectrum produced in a background region near the peak. For the 269 keV decay from the 10^+ isomer a half-life $T_{1/2}(10^+) = 7.5(3)$ μs (Fig. 3 top) is found, in good agreement with the earlier reported value of 7.7(5) μs [25,26]. The decay curve of the 7^- isomeric level consists of two components: the direct decay from 7^- isomers implanted at $t = 0$ and the growth-decay curve originating from 10^+ isomers decaying into the lower one after implantation. The two component fit of the time spectrum of the 909 keV + 1141 keV, performed by keeping the half-life of the upper 10^+ isomer fixed, allowed the half-life of $T_{1/2}(7^-) = 5.9(8)$ μs (Fig. 3 bottom) and the ratio of the direct isomer population $N_7/N_{10} = 0.9(2)$ to be determined. The deduced half-life is in good agreement with the previously reported value 6.6(1.4) μs [6].

For the g factor determination the time-differential perturbed angular distribution (TDPAD) method [9] has been used. The background-corrected and normalized time spectra measured for the two field directions (up and down), are combined to produce the experimental $R(t)$ spectrum:

$$R_{exp}(t) = \frac{Y(t, B_{up}) - Y(t, B_{down})}{Y(t, B_{up}) + Y(t, B_{down})} \quad (1)$$

Time spectra gated on the 909 keV and 1141 keV transitions registered at the angles $\theta = \pm 45$ and $\theta = \pm 135$, with respect to the beam direction have been used to create an $R(t)$ spectrum with maximum amplitude (see [21] for details). The oscillation amplitude of the $R(t)$ spectrum created with the detectors placed at $\theta = \pm 75$ and $\theta = \pm 105$ is reduced by a factor of two compared to that of the $R(t)$ created with detectors in the geometry $\theta = \pm 45$ and $\theta = \pm 135$. In the present experimental conditions, characterized by a rather low degree of the nuclear alignment (see below), the $R(t)$ spectrum corresponding to the detectors placed at $\theta = \pm 75$ and $\theta = \pm 105$ did not evidence any oscillation, and therefore these data were not included in the analyses.

In the present case two cascade decaying isomeric levels with comparable half-lives are simultaneously populated in the nuclear reaction. The modulation ratio corresponding to γ rays that depopulated the upper 10^+ isomeric state could not be fitted due to the low statistics for the 269 keV γ ray. The g factor of the 10^+ state has been assumed to be $g(10^+) = -0.243$ (the average value measured for the $11/2^-$ states in the neigbouring odd isotopes [27] with a similar $(\nu h_{11/2})$ hole configuration). The g factors for the 10^+ state have been measured in ^{116}Sn and ^{118}Sn, with values of $-0.2326(15)$ and $-0.2447(7)$, respectively, and they agree within 7% with the g factors of the $11/2^-$ states in neighbouring odd-mass Sn [27]. A shell-model calculation [20,29] predicts $g_{SM}(10^+) = -0.238$, agreeing well with this estimated value. The $R(t)$ ratio for the 269 keV γ ray, constructed with a time calibration appropriate to observe the fast Larmor oscillations corresponding to the expected g factor, has large statistical errors, about 0.15 (three times larger than the errors of the $R(t)$ for 909 + 1141 keV, see Fig. 4 below). These large errors prevented the observation of low amplitude oscillations corresponding to the small alignment degree of this experiment (see below).

The experimental $R(t)$ spectrum for the sum of 909 and 1141 keV γ rays de-exciting the lower lying 7^- isomer is illustrated in Fig. 4a. In this case the modulated intensity is composed of two contributions: the cascade component coming from the 10^+ state and the direct component coming from the reaction. The calculated modulation ratio, depending on the Larmor frequencies ω_{10} and ω_7 that are describing the precession in the states 10^+ and 7^-, respectively, has the form (see Ref. [28]):

$$R(t) = \frac{b_2}{1 + A(t)} \cos 2(\theta - \omega_7 t) + \frac{A(t)}{1 + A(t)} R_{casc}(t, \omega_7, \omega_{10}) \quad (2)$$

where

$$R_{casc}(t, \omega_7, \omega_{10}) = b_2 \cos\alpha \left[\cos\left[2(\theta - \omega_{10} t) - \alpha\right)\right] + 2\left(1 - e^{\Delta\lambda t}\right)^{-1} \sin\left[2\theta - (\omega_7 + \omega_{10})t - \alpha\right] \sin \Delta\omega t \quad (3)$$

and

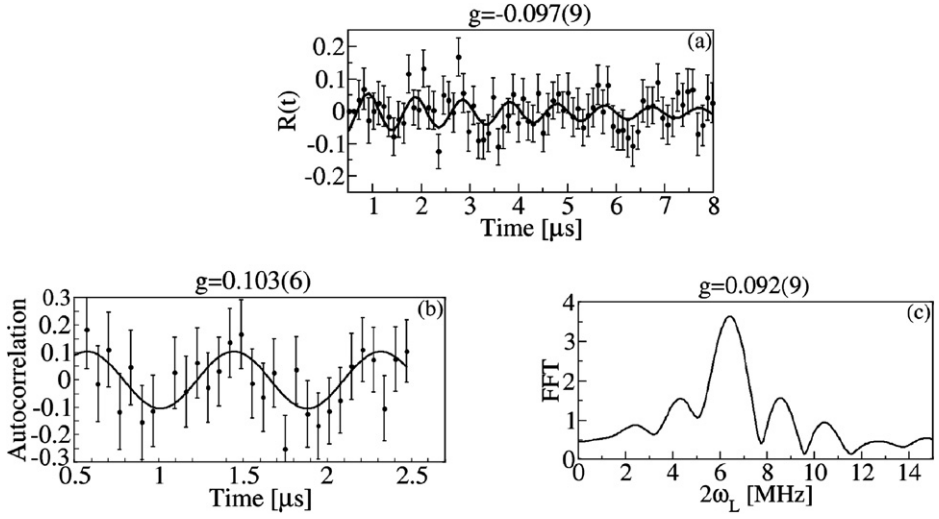

Fig. 4. The direct fit of the $R(t)$ function for $(909 + 1141)$ keV transitions in ^{126}Sn (a), autocorrelation analysis (b) and Fast Fourier Transform result (c).

$$A(t) = \frac{N_{10}}{N_7}\frac{\lambda_{10}}{\Delta\lambda}\left(e^{\Delta\lambda t} - 1\right)$$

$$\Delta\lambda = \lambda_7 - \lambda_{10}, \quad \text{with} \quad \lambda_i = \frac{\ln 2}{T_{1/2}}$$

$$\Delta\omega = \omega_7 - \omega_{10}$$

$$\alpha = \arctan(2\Delta\omega/\Delta\lambda)$$

The values for the decay constants λ_{10} and λ_7 and the ratio N_7/N_{10} of the population of the two isomeric levels have been extracted from the lifetime analysis. The amplitude of the oscillation b_2 is given by $b_2 = \frac{3}{4}A_2$, where A_2 is the angular distribution coefficient dependent on the transition type and on the degree of spin alignment. The same coefficients b_2 were assigned to the direct and cascade decays, assuming identical alignments for the two isomers.

The contribution of the term R_{casc} was dramatically reduced in our case on account of the $\cos\alpha$ factor, which for the large applied magnetic field of 7 kG took a value of 0.0008. Therefore for fitting the experimental $R(t)$ only the first term in expression (2) was used, with the amplitude b_2 and the Larmor frequency $\omega_7 = \frac{g(7^-)B\mu_n}{\hbar}$ as free parameters. As seen in Fig. 4a, the observed damping is well accounted for by the time-dependent amplitude $\frac{1}{1+A(t)}$. From the least-squares analysis of the modulation curve, the g factor of the 7^- isomer $g(7^-) = -0.097(9)$, and the amplitude $b_2 = 0.07(3)$, have been derived.

Since the period of the Larmor precession (~ 1 μs, see Fig. 4a) is shorter than the lifetime of the isomer (5.9(8) μs), an autocorrelation analysis was performed [16]. The calculated autocorrelation function ($ACF(n)$) has the form:

$$ACF(n) = \sum_{k=k_1}^{k_2-n} \frac{f(k)f(k+n)}{k_2-k_1-n} \Bigg/ \sum_{k=k_1}^{k_2} \frac{f^2(k)}{k_2-k_1} \tag{4}$$

where $f(k)$ represents the experimental data as a function of the channel number k, $k_2 - k_1$ is the observation window and n is the folding back window ($n \ll k_2 - k_1$). The information from a 7 μs window have been folded back into a 2 μs time window (see Fig. 4b). In the present experimental conditions and due to the smearing out of the oscillation pattern after 8 μs only data up to 7 μs have been included in the autocorrelation analysis to obtain the optimal amplitude. If data from later times are included the amplitude of the autocorrelation function is reduced. Fitting the autocorrelation data leads to a g-factor value of 0.103(6), which is in good agreement with the value obtained from fitting the raw $R(t)$, see Fig. 4b. Note that in this case phase and amplitude have no longer a physical meaning.

As a last step, we have performed a Fast Fourier analysis (FFT), which reveals a peak at $2\omega_L = 6.2(6)$ MHz (Fig. 4c), corresponding to a g factor of 0.092(9), in agreement with the values deduced by the other analysis procedures.

As a final value, we adopt the mean from the different analysis procedures, resulting in $g(7^-) = -0.098(9)$.

Table 1
Experimental g factor for the 7^- isomer in even mass Sn isotopes compared to shell-model calculations.

Isotope	E_x (keV)	$T_{1/2}$	g_{exp}	g_{free}	g_{eff}[1]	g_{cp}[2]
^{114}Sn	3088	765 ns	−0.0806(5)[3]			
^{118}Sn	2575	217 ns	−0.0978(6)[3]			
^{126}Sn	2219	5.9 μs	−0.098(9)	−0.081	−0.057	−0.082
^{128}Sn	2092	6.5 s		−0.076	−0.054	−0.070
^{130}Sn	1947	1.7 m	−0.0544(4)[4]	−0.067	−0.048	−0.048

[1] SM $g_s(\nu) = -2.513$ and $g_l(\nu) = -0.0039$.
[2] SM corrected for A dependence of core polarization.
[3] Ref. [33].
[4] Ref. [34].

In Table 1 this value has been compared to the g factors of other 7^- states in even-Sn isotopes with main quasi-particle configuration $(h_{11/2}^{-1}d_{3/2}^{-1})$. The Schmidt value for this configuration is $g_{schmidt} = -0.11$, which is close to the observed experimental values and confirms that this is the leading configuration of these isomers. The extreme sensitivity of $g(7^-)$ to small components in the wave function due to the partial cancellation of the $d_{3/2}$ and $h_{11/2}$ contributions of opposite sign allows a more detailed discussion. Extended untruncated shell-model calculations in the full $N = 50$–82 neutron space $(g_{7/2}, d_{5/2}, d_{3/2}, s_{1/2}, h_{11/2})$, were recently performed for the whole Sn region down to ^{124}Sn, using a realistic two-body interaction based on the CD-Bonn interaction and ^{88}Sr as a core [20,29]. The obtained g factors using free and effective single nucleon values are given in Table 1. Effective neutron g factors $g_s = -2.513$ and $g_l = -0.0039$ were adjusted to the experimental single hole values for $d_{3/2}$ and $h_{11/2}$ in ^{131}Sn. Fair agreement with experiment is observed from ^{130}Sn to ^{126}Sn, but the increase of $|g|$ with increasing distance from ^{132}Sn is only qualitatively reproduced. Note that for ^{126}Sn a slightly better agreement is observed if free g factors are used, which will be further discussed. Moreover, additivity of g factors is consider-

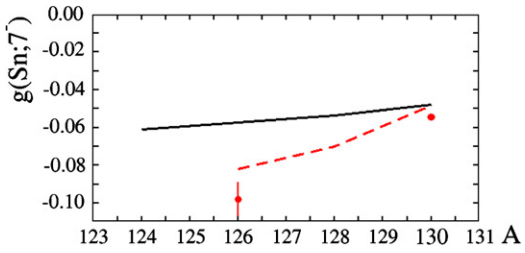

Fig. 5. g Factors for $I^\pi = 7^-$ states in even Sn isotopes. The full line represent g_{eff} and the dashed g_{cp} from Table 1. Directly measured values (red circles) are compared to SM results. The error on the g factor in ^{130}Sn is smaller than the symbol size. (For interpretation of the references to colour in this figure legend, the reader is referred to the web version of this Letter.)

ably violated for ^{130}Sn and ^{126}Sn, yielding values of $-0.0756(10)$ and $-0.0826(10)$, respectively, as calculated from the experimental $g(3/2^+)$ and $g(11/2^-)$ in the neighboring odd-A isotopes. These values are nicely reproduced using shell-model values for the $3/2^+$ and $11/2^-$ states, yielding additivity values of -0.076 and -0.077 for ^{130}Sn and ^{126}Sn. These values, however, are quite different from the calculated $g(7^-)$ (see Table 1), indicating that admixtures of different origin appear in the $I^\pi = 7^-$ and the $I^\pi = 3/2^+$, $11/2^-$ wave functions. The respective components amount to less than 2% of the wave function, yet they have a strong influence on the calculated moments.

The too weak A dependence of the shell model $g(7^-)$ values may be due to the fact that a common effective operator cannot account for partial blocking of core polarization with increasing distance from ^{132}Sn as this is not covered by the present valence space. The main core polarization configurations for the M1 operator in this region are the neutron $\nu(h^{-1}_{11/2}h_{9/2})$ and the proton $\pi(g^{-1}_{9/2}g_{7/2})$ $N = 82$ and $Z = 50$ cross-shell excitations [30] besides the $\nu(d^{-1}_{5/2}d_{3/2})$ which is included in the shell-model valence space. Corrections due to the A dependence (blocking and mixing) of core-excited configurations were calculated with an interaction and valence space used recently for core excited states in ^{132}Sn and ^{131}In [4]. Free nucleon g factors were used which account for the experimental $\nu d_{3/2}$ and $\nu h_{11/2}$ g factors in ^{131}Sn. The results are shown in the last column of Table 1 and account very well for the experimental g factor trend (Fig. 5). Core polarization amounts to 4.8% (^{130}Sn) to 2.5% (^{126}Sn) of the wave function, confirming the increased blocking as one moves away from ^{132}Sn. The corrections should be regarded as a trend estimate, as they were obtained in a different model space with a different interaction. We note that this approach also reproduces the absolute values and A dependence of the $d_{3/2}$ and $h_{11/2}$ quasi-particle states in $^{125-131}$Sn. All shell model results in the present work were performed with the code OXBASH [31].

Apart from extracting the g factor for this isomeric state, another goal of this work was to establish whether and how much alignment can be produced in a relativistic fission reaction. The amplitude of the experimental $R(t)$ curve (Fig. 4a) is indeed related to the amount of alignment that is present in the implanted ensemble of isomers [18]. From the experimental amplitude $b_2 = 0.07(3)$, and considering the angular distribution coefficient for total alignment $A_2^{\max} = 0.51$ [32] for the stretched E2 cascade $(4 \to 2 \to 0)$, we find an alignment $A = 18(8)\%$. Herewith, we have proven for the first time that isomers produced in a relativistic fission reaction and subsequently selected as fully-stripped ions through a fragment separator, are aligned and can maintain their alignment during the in-flight selection process. The observed amount is similar to that observed for fragments produced in an intermediate- or high-energy projectile fragmentation reaction (order of 10–20%).

In conclusion, for the first time a spin-aligned isomeric ensemble was observed in a relativistic-fission reaction. A comparison with the shell-model calculation for the g factor of the 7^- state in ^{126}Sn supports the assigned configuration and reveals details on small admixtures in the wave functions both from inside and outside the pure neutron model space. The amount of spin alignment deduced from this experiment and the fact that it can be maintained during the in-flight selection process, opens the possibility for further investigations on electromagnetic moments of exotic nuclei produced in relativistic fission.

Acknowledgements

This work was performed using the grant 06KY205I of the BMBF (Germany), IAP contract P6/23 of BELSPO (Belgium) and GO446-05 of FWO Vlaanderen, the Polish Ministry of Science and Higher Education (Grant 1-P03B-030-30), the Romanian National Authority for Scientific Research contract IDEI 52/07, the Bulgarian National Science Fund grant No. VUF06/05 and by the European Commision Contract No. RII3-CT-2004-506065. We acknowledge the technical support received from the GSI accelerator facility.

References

[1] J. Dobaczewski, et al., Phys. Rev. C 53 (1996) 2809.
[2] T. Kautzsch, et al., Eur. Phys. J. A 9 (2000) 201.
[3] A. Jungclaus, et al., Phys. Rev. Lett. 99 (2007) 132501.
[4] M. Górska, et al., Phys. Lett. B 672 (2009).
[5] J. Pinston, J. Genevey, J. Phys.: Nucl. Part. Phys. 30 (2004) R57.
[6] B. Fogelberg, et al., Nucl. Phys. A 323 (1979) 205.
[7] M. Mineva, et al., Eur. Phys. J. A 11 (2001) 9.
[8] Z. Podolyak, et al., Phys. Lett. B 632 (2006) 203.
[9] K. Alder, R.M. Steffen, Annu. Rev. Nucl. Sci. 14 (1964) 403.
[10] G. Neyens, Rep. Prog. Phys. 66 (2003) 633.
[11] W.-D. Schmidt-Ott, et al., Z. Phys. A 350 (1994) 215.
[12] J.B. Wilhelmy, et al., Phys. Rev. C 5 (1972) 2041.
[13] A. Wolf, et al., Phys. Rev. Lett. 36 (1976) 1072.
[14] H. Geissel, et al., Nucl. Instrum. Methods Phys. Res. B 70 (1992) 286.
[15] O.B. Tarasov, D. Bazin, Nucl. Instrum. Methods B 266 (2008) 4657.
[16] G. Georgiev, et al., J. Phys. G 28 (2002) 2993.
[17] K. Asahi, et al., Phys. Rev. C 43 (1991) 456.
[18] I. Matea, et al., Phys. Rev. Lett. 93 (2004) 142503.
[19] Th. Schwab, GSI report 91-10, 1991.
[20] R. Lozeva, et al., Phys. Rev. C 77 (2008) 064313.
[21] G. Neyens, et al., Acta Phys. Pol. 38 (2007) 1237.
[22] M. Mineva, PhD thesis, University of Lund, 2004.
[23] J. Eberth, et al., Nucl. Instrum. Methods Phys. Res. A 369 (1996) 135.
[24] J. Grębosz, Comput. Phys. Commun. 251 (2007) 176.
[25] J. Genevey, et al., in: B.M. Sherill, D.L. Morrissey, C.N. Davids (Eds.), Exotic Nuclei and Atomic Masses, AIP, New York, 1998, p. 694.
[26] C.T. Zhang, et al., Phys. Rev. C 62 (2000) 057305.
[27] N.J. Stone, Atomic Data and Nuclear Data Tables 90 (2005) 75.
[28] M. Ionescu-Bujor, et al., Nucl. Phys. A 272 (1976) 1.
[29] H. Grawe, in press, 2010.
[30] B.A. Brown, et al., Phys. Rev. C 71 (2005) 044317.
[31] B.A. Brown, et al., Oxbash for windows, MSU-NSCL report 1289, 2004.
[32] T. Yamazaki, Nucl. Data A 3 (1967) 1.
[33] M. Ishihara, et al., in: J. de Boer, H.J. Mang (Eds.), Proccedings of the International Conference on Nuclear Physics, vol. 1, North-Holland, Amsterdam, 1973, p. 256.
[34] F. le Blanc, et al., Phys. Rev. C 72 (2005) 034305.